Phenomenological Predictions of Cohesive Energy and Structural Transition of Nanoparticles

S. C. Vanithakumari and K. K. Nanda*

Materials Research Centre, Indian Institute of Science, Bangalore, 560 012, India

Received: October 3, 2005

In this paper, it is shown that a liquid-drop model (LDM) can predict the size-dependent cohesive energy (SDCE) of large nanoparticles and clusters (particles with few atoms) quantitatively. The cohesive energy decreases linearly with the inverse of the particle size both for large nanoparticles and clusters though the slopes are different. This indicates that there are three different regions (I−III) of SDCE in the complete size range. Regions I and II represent the SDCE of large nanoparticles and clusters, respectively, while region II represents the intermediate region where the cohesive energy is almost size-independent. Different regions of SDCE correspond to different structures of nanoparticles, and structural transition associated with the particle size can easily be predicted from the SDCE. Analyzing the cohesive energy data on the basis of LDM, it is shown that the surface tension decreases with decreasing size for very small nanoparticles. The Tolman equation can account for the variation of surface tension by predicting the size dependency of the Tolman length.

Cohesive energy is one of the important physical quantities that quantify the thermal stability of the materials such as melting temperature, boiling temperature, solubility, and so forth. It has been well established both experimentally and theoretically that the cohesive energy and the melting temperature of nanoparticles with relatively free surface decreases with decreasing particle size. The boiling temperature is also predicted to decrease with decreasing particle size, and the solubility is shown to be higher. Liquid-drop model (LDM) has been used for the quantitative understanding of the size-dependent cohesive energy (SDCE) and separation energy of clusters (particles with few atoms).[1,2] LDM has also been used to understand[3−6] the size-dependent lattice parameter (SDLP), the size-dependent melting (SDM), and the size-dependent evaporation (SDE) of large nanoparticles (particles larger than 5.0 nm). Though LDM has successfully been used to understand the SDCE of clusters,[1] it overestimates the cohesive energy of Mo and W nanoparticles.[7] Apart from the LDM, there are other different models that predict the SDCE of nanoparticles.[7−14] According to all theoretical models, the cohesive energy of free nanoparticles decreases linearly with the inverse of the particle size. The bond energy (BE) model,[7−9] the surface area difference (SAD) model,[10] and the thermodynamic model[11] predict experimental SDCE data[15] of Mo and W nanoparticles, quantitatively. However, all these models underestimate the cohesive energy of clusters. On the basis of the bond-order-length-strength (BOLS) mechanism, Sun et al.[12b] have predicted the SDCE and size-dependent melting temperature in the complete size range. Both the cohesive energy and the melting temperature of Ga, Sn, C, and Si clusters are predicted to be higher than the bulk value. In contrast, molecular dynamics (MD) simulations[16] as well as experimental data[1d] reveal that the cohesive energy of Si clusters is less compared to that of bulk. Therefore, the validity of the BOLS mechanism, especially for cohesive energy of clusters, is questionable though it is consistent with experimental data[17] and MD simulations[16] on the superheating of Sn clusters. Overall, no models can predict or explain the SDCE in the complete size range.

In this paper, it is shown that LDM can explain the SDCE in the complete size range by predicting the cohesive energy of nanoparticles and clusters, quantitatively. In almost all cases, a higher surface tension as compared to the bulk value is obtained when the SDLP or SDE data is compared with LDM.[3−6] In ref 7, the cohesive energy of nanoparticles has been evaluated by using the bulk surface tension and is shown to overestimate the cohesive energy of Mo and W nanoparticles. To avoid any confusion, we refer to the bulk surface tension as γ and to the value obtained from SDLP and SDE as the surface tension of nanoparticles γ_n. We also refer to very small nanoparticles (∼1 nm) as clusters. First of all, a correlation between γ_n and γ is established by analyzing the SDE and SDM of nanoparticles on the basis of LDM. By using the relation between γ_n and γ, γ_n is calculated and used for the quantitative understanding of cohesive energy of Mo and W nanoparticles. Second, the size-dependent cohesive energy (SDCE) of nanoparticles and clusters is shown to have three different regions in the complete size range that is obtained by analyzing the experimental data on the basis of LDM. Different regions correspond to different structures of nanoparticles, and structural transition (ST) associated with the particle size can easily be predicted from the SDCE. It is also shown that γ_n decreases with decreasing size of very small nanoparticles. The Tolman equation[18] can account for the variation of γ_n by predicting the size dependency of the Tolman length.

Now, we discuss the SDCE of nanoparticles on the basis of different theoretical models. In refs 7 and 8, the expression for the SDCE has been derived by assuming the shape of the nanoparticles as cube. If the shape is assumed to be spherical, the variation of SDCE will be different.[9] Further, it is not clear why the cohesive energy per surface atom (a_{vc}) should be 4 times less than the cohesive energy per interior atom (a_v). The cohesive energy of surface atom (a_{vc}) is related to the cohesive energy of interior atom (a_v) as[14]

$$a_{vc} = (z_s/z_b)^{1/2} a_v \quad (1)$$

* Author to whom correspondence should be addressed. E-mail: nanda@mrc.iisc.ernet.in.

10.1021/jp055617n CCC: $33.50 © 2006 American Chemical Society
Published on Web 12/17/2005

The coordination number (z_b) of interior atoms of bcc crystals is 8, whereas the coordination number (z_s) of surface atoms is 4, which implies that $a_{vc} \sim 0.707a_v$. Similarly, the coordination number of surface atoms of fcc crystals is 8, whereas that of interior atoms is 12 implying that $a_{vc} \sim 0.817a_v$. Assuming that the reduction in cohesive energy is mainly due to the surface layers, the cohesive energy of nanoparticles is represented as[7−9,14]

$$a_{v,d} = a_v\left(1 - \frac{N_s}{N}\right) + \frac{N_s}{N}a_{vc} \tag{2}$$

Substituting eq 1 in eq 2, the cohesive energy of nanoparticles $a_{v,d}$ can be expressed as

$$a_{v,d} = a_v\left[1 - \frac{N_s}{N}\left(1 - \sqrt{\frac{z_s}{z_b}}\right)\right] \tag{3}$$

For cubic-shaped nanoparticles, $N_s/N = 12r_a/d$, where r_a is the atomic radius and d is the particle diameter, while $N_s/N = 8r_a/d$ for spherical nanoparticles. This indicates that cohesive energy decreases rapidly for cubic-shaped nanoparticles when compared with spherical nanoparticles. Further, the ratio between a_v and a_{vc} is different for different crystal structures implying that the variation of cohesive energy of bcc and fcc nanoparticles is different. Irrespective of the crystal structure of the nanoparticles, eq 3 overestimates the cohesive energy of nanoparticles. However, if we substitute $a_{vc} = a_v/4$ as is the case for the BE model, the expression for $a_{v,d}$ will be identical to that obtained from the BE model, and eq 3 can account for the SDCE of Mo and W nanoparticles, quantitatively.

According to LDM,[1,4] the total cohesive energy (E_b) of a nanoparticle of N atoms is equal to the volume energy a_vN minus the surface energy $4\pi r_a^2N^{2/3}\gamma$, the later term arising from the presence of atoms on the surface. Hence, the mean cohesive energy per atom of a nanoparticle, that is, $E_b/N = a_{v,d}$ is given by[1,4]

$$a_{v,d} = a_v - \frac{4\pi r_a^{\,2}\gamma_n}{N^{1/3}} \tag{4}$$

where a_v represents the cohesive energy of bulk, and r_a is the radius of one atom deduced from the atomic volume ($v_0 = 4\pi r_a^3/3$). The number of atoms in a spherical nanoparticle of diameter "d" being

$$N = \frac{d^3}{(2r_a)^3}$$

the expression for the mean cohesive energy per atom of a nanoparticle becomes

$$a_{v,d} = a_v - \frac{6v_0\gamma_n}{d} \Rightarrow \frac{a_{v,d}}{a_v} = 1 - \frac{6v_0\gamma_n}{a_v d} \tag{5}$$

The variation of the cohesive energy is linear with the inverse of the particle size. This is consistent with the experimental results[1,15] and with the other theoretical models.[7−14] According to the Wulff construction,[19,20] γ_n/d is constant for all crystal faces of a faceted nanoparticle, even though the surface energy is different, indicating that eq 5 holds for all crystal faces. Further, eq 5 also holds for cubic-shaped nanoparticles which is expected as the surface-to-volume ratio is the same for spherical nanoparticles. In contrast, the variation of cohesive energy of nanocubes and spherical nanoparticles is predicted to be different by the BE model.[7−9] Experimental investigation is required to shed light on this issue. Before we analyze the experimental data using LDM, it is compared with the recently developed SAD model[10] and the thermodynamic model[11] for Ag and Au as shown in Figure 1a and b. These two materials are chosen as their γ_n of free nanoparticles is available in the literature.[5,6] LDM is consistent with the SAD model[10] and the

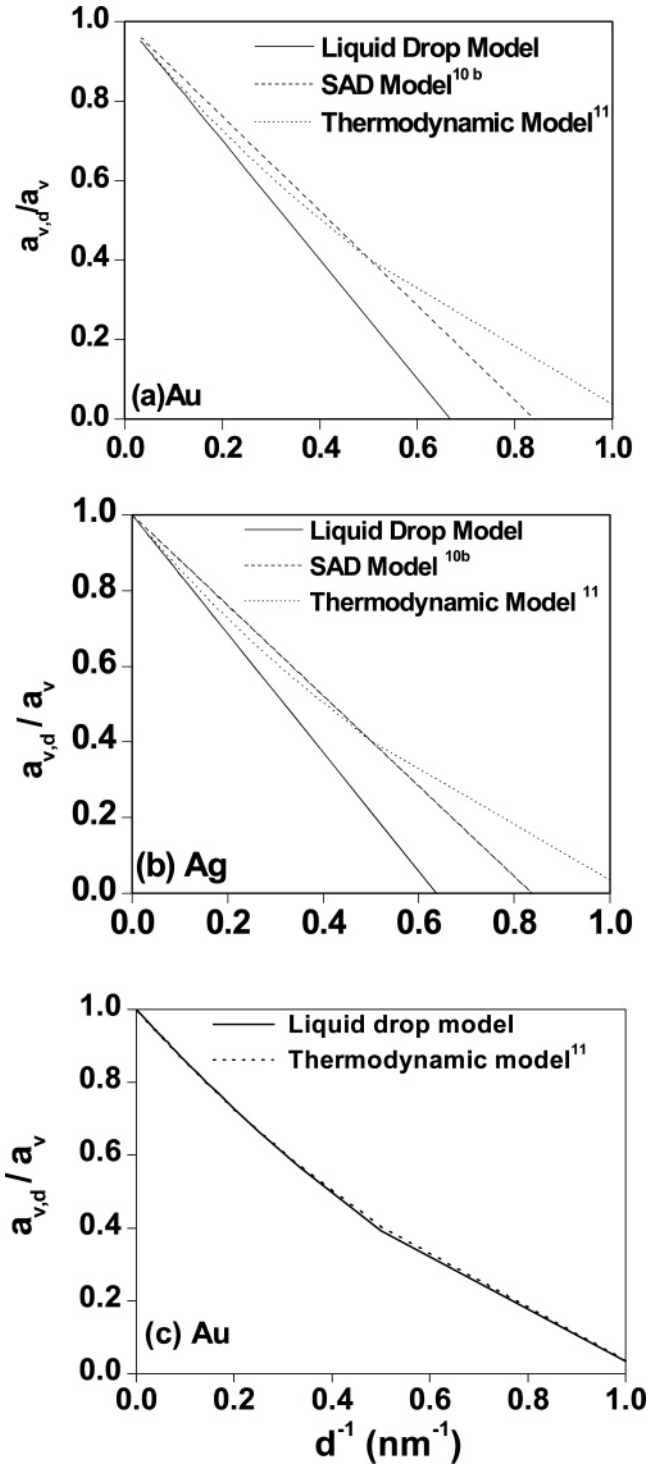

Figure 1. Comparison of cohesive energy of (a) Ag and (b) Au nanoparticles predicted by different theoretical models. (c) SDCE of Au nanoparticles predicted by LDM with size-dependent surface tension and thermodynamic model. The size-dependent surface tension is calculated on the basis of the Tolman equation with a Tolman length of 0.085 nm.

TABLE 1: Comparison of Surface Tension of Ag Nanoparticles Reported in the Literature[5,21−27]

surroundings	γ_n (J/m^2)	methods	ref
cellulose membrane	6.56	SDLP	21
surface oxidation	5.96	SDLP	22
on carbon substrate	6.405/1.415	SDLP	23
solid argon	2.286	SDLP	24
soda-lime glass	4.7	SDLP	25
nearly free	6.3	SDLP	25
on carbon substrate	1.13	evaporation study	26
glass/quartz	6.0	evaporation study	27
free	7.2	SDE	5

TABLE 2: Comparison of Surface Tension of Au Nanoparticles Reported in the Literature[6,28−32]

surroundings	γ_n (J/m^2)	methods	ref
on carbon substrate	1.175	SDLP	28
on carbon substrate	3.19	SDLP	29
in a polymer matrix[a]	6.3 (6.71)	SDLP	30
ligand stabilized[a]	7.2 (7.70)	SDLP	30, 31
on carbon substrate	1.42	evaporation study	32
free	8.78	SDE	6

[a] The values are obtained by taking $\kappa = 6.23 \times 10^{-12}$ m^2/N,[30] whereas the bracketed values are obtained by taking $\kappa = 5.85 \times 10^{-12}$ m^2/N.[28]

thermodynamic model[11] for large nanoparticles that predict a linear relation between cohesive energy and the inverse of the particle size. However, the thermodynamic model deviates from the linearity for smaller nanoparticles/clusters. LDM can predict a similar variation of SDCE by assuming the variation of surface tension according to the Tolman equation (Figure 1c) with a Tolman length of 0.085 nm.

According to the Tolman equation,[18] γ is almost size-independent for large nanoparticles and decreases with decreasing particle size d for very small particles. In view of that, γ_n should be equal to γ for large nanoparticles. In contrast, γ_n obtained from SDLP and SDE data is much higher compared to γ. A wide value of γ_n for Ag[5,21−27] and Au[6,28−32] nanoparticles has been reported in the literature, and the values are compiled in Tables 1 and 2, respectively. Different values of γ_n have been obtained both for Ag and for Au (Tables 1 and 2). Alivisatos and co-workers[33] have obtained $\gamma_n = 2.5$ J/m^2 for bare CdS nanoparticles and $\gamma_n = 1.74$ J/m^2 for capped CdS nanoparticles from SDLP while $\gamma = 0.75$ J/m^2. Also as noted from Table 2, γ_n of Au obtained from the evaporation as well as from the SDLP studies is different for different substrates. Thus, the difference in γ_n for Au and Ag is believed to be due to the different surroundings or to the different particle−substrate interaction. In refs 5 and 6, γ_n of free nanoparticles has been evaluated by analyzing the SDE data on the basis of the Kelvin effect and the LDM. However, γ is used in the LDM to understand SDM of nanoparticles. Therefore, we compare SDM and SDE of free nanoparticles to examine a correlation between γ_n and γ.

The SDE data[5,6] is obtained by monitoring the onset temperature of evaporation (T_{onset}) as a function of d where T_{onset} is the temperature at which d decreases as a consequence of the partial evaporation. By plotting the onset temperature of evaporation (T_{onset}) against $1/d$, the evaporation temperature ($T_{onset,b}$) of bulk material is extrapolated.[5,6] On the basis of the SDE data of Ag and Au, the slope of $T_{onset}/T_{onset,b}$ versus $1/d$ is evaluated to be 1.05 and 0.94 nm for Ag and Au, respectively.[5,6] According to LDM,[6] the slope of T_m/T_{mb} versus $1/d$ curve is predicted to be 0.97 and 1.13 nm for Ag and Au, respectively, and is nearly the same as that obtained from $T_{onset}/T_{onset,b}$ versus $1/d$. Here, T_m represents the melting temperature of nanoparticles and T_{mb} represents the bulk melting temperature. Though the slopes of SDE and SDM are nearly equal, SDE data[5,6] yields $\gamma_n = 7.20$ and 8.78 J/m^2 for Ag and Au, respectively, while γ of 1.065 and 1.363 J/m^2 is used to predict the SDM[4] of Ag and Au nanoparticles, respectively. In this context, cohesive energy per atom is obtained from the SDE data, whereas cohesive energy per coordination is scaled to the melting temperature to evaluate SDM.[4] For fcc crystal structure, the cohesive energy per coordination is 6 times lower than the cohesive energy per atom. This is because the coordination number of an fcc crystal lattice is 12 and each bond is shared by two atoms. Thus, γ_n is expected to be 6 times higher than γ and is in excellent agreement with the values obtained from the SDE data. This indicates that γ_n is related to γ in the same way as the cohesive energy per atom is related to the cohesive energy per coordination. This yields $\gamma = 1.20$ and 1.46 J/m^2 for Ag and Au, respectively, which is in excellent agreement with the values reported for the bulk[34,35] and strengthens the relation between γ and γ_n which is given by[36]

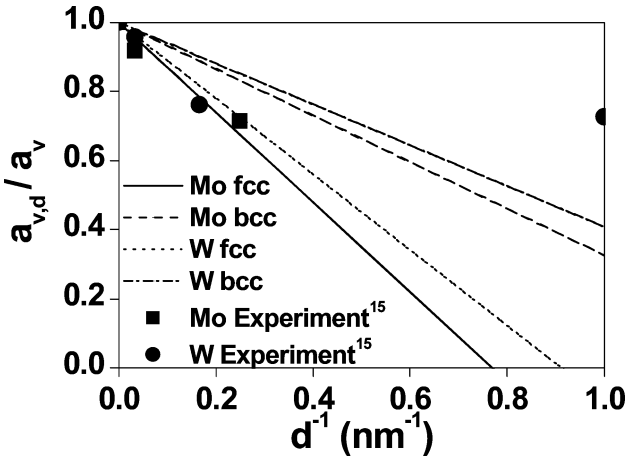

Figure 2. Comparison of cohesive energy of Mo and W nanoparticles with LDM. $\gamma_n = 4\gamma$ for bcc and $\gamma_n = 6\gamma$ for fcc structure.

$$\gamma_n = C\gamma/2 \tag{6}$$

As the coordination number of materials with fcc, bcc, sc, and diamondlike crystal structure is 12, 8, 6, and 4, respectively, γ_n will be 6, 4, 3, and 2 times higher than γ. This relation also holds for NaCl type crystals such as PbS[36] which proves its validity for other materials. For particles larger than 5.0 nm, the coordination number can be considered as that of bulk, implying that the surface tension is size-independent. However, the coordination number and, hence, the surface tension are expected to decrease with particle size for small particles.[37]

Both Mo and W nanoparticles undergo ST from bcc to fcc when the crystallite size is smaller.[14] Further, γ_n cannot be deduced conclusively as there are few data points. Therefore, we calculate γ_n by using eq 3, and then we calculate the SDCE for comparison with experimental data. As γ is 2.907 J/m^2 of Mo,[35] γ_n is calculated to be 11.63 and 17.44 J/m^2 for bcc and fcc structure, respectively. Similarly, γ is 3.265 J/m^2 for W and γ_n is calculated to be 13.06 and 19.59 J/m^2 for bcc and fcc W, respectively. On the basis of the above discussion on the relation between γ and γ_n, we evaluate the cohesive energy of Mo and W nanoparticles and compare with the experimental data as shown in Figure 2. We have taken the bulk cohesive energy of bcc Mo and W as 6.83 and 8.81 eV and that of fcc Mo and W as 6.45 and 8.43 eV, respectively.[14] LDM overestimates the

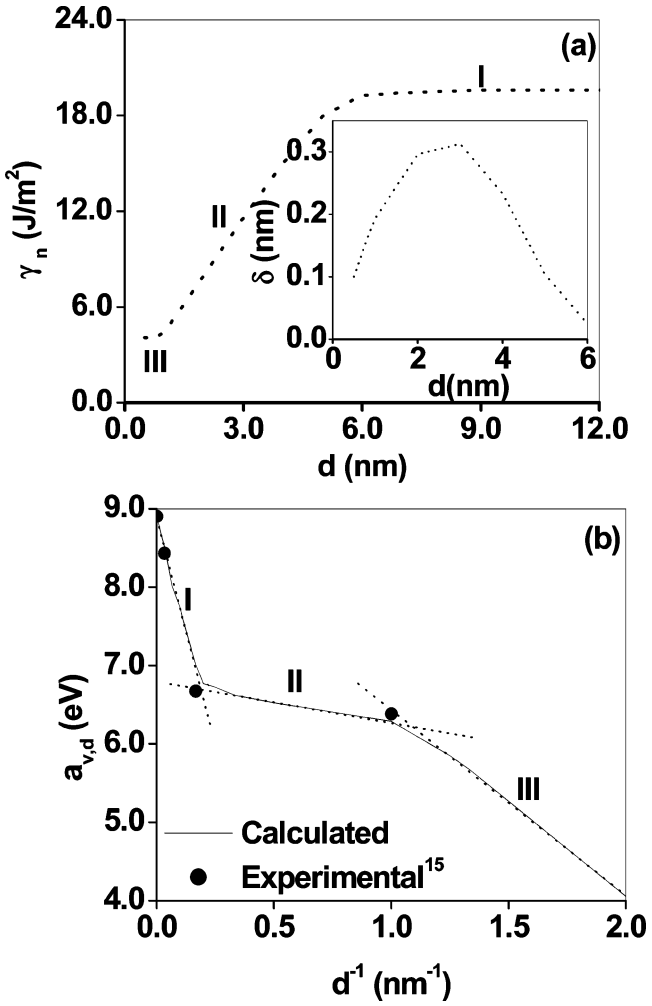

Figure 3. (a) Fabricated size-dependent surface tension of nanoparticles. Inset shows the Tolman length estimated from the size-dependent surface tension by using the Tolman equation. (b) Size-dependent cohesive energy of nanoparticles calculated by using the size-dependent surface tension of nanoparticles. ST can be deduced by employing an interpolation procedure as demonstrated in the figure.

cohesive energy of nanoparticles with bcc structure but explains the cohesive energy of nanoparticles with fcc structure. The disagreement between the LDM and the cohesive energy of nanoparticles with bcc structure may be due to the difference in the coordination number of bcc Mo and W. In the case of Mo and W with bcc crystal structure, the effective coordination number[14] is 5.6 and γ_n of bcc is close to that of fcc.

Now, we discuss the SDCE of clusters. Though the BE model[7,8] and the thermodynamic model[11] explain the SDCE of nanoparticles quantitatively, they cannot be applied for clusters. However, LDM has successfully been used to understand the SDCE of clusters,[1] and it can also be applied to large nanoparticles. The only difference is that $\gamma_n = C\gamma/2$ can explain the SDCE of large nanoparticles while γ_n between γ and 2γ is obtained from the SDCE of clusters.[1,38−40] The difference may be due to the variation of coordination number with size. To account for the SDCE of W clusters, we fabricate the size-dependent coordination number and calculate the size-dependent surface tension for W as shown in Figure 3a. Similar variation of surface tension is also predicted by Monte Carlo simulation.[41] In regions I and III, the coordination number is taken as 12 and 2.5 and is considered to be size-independent. The coordination number for clusters (region III) is assumed to be size-independent as γ is obtained from the SDCE of clusters.[1] However, the coordination number decreases with decreasing particle size in region II. This indicates that the surface tension is size-independent for large nanoparticles (region I), as is the case[36] for Au, Ag, and PbS, as well as for clusters (region III), as is the case[1] for Na, K, and Cs, while the surface tension decreases with decreasing particle size in region II.

The size dependency of surface tension reminds us that the Tolman equation[18] predicts that surface tension should decrease with decreasing particle size. On the basis of Figure 3a, we estimated the Tolman length δ, and we found it to be size-dependent as shown in the inset of Figure 3a. δ is zero for large nanoparticles and increases with decreasing particle size. The maximum value of δ is 0.31 nm and is of the order of the atomic diameter. When the particle size is reduced further, δ decreases. In the limit of particle size approaching zero, δ is expected to be zero. Overall, it is predicted that the surface tension of nanoparticles is almost size-independent for large nanoparticles (region I) and decreases with decreasing size in the intermediate size range (region II). In this context, many theoretical models[42] predict δ to be negative in region I which indicates that the surface tension should decrease with increasing size. However, the value of δ is so small that the surface tension can be considered size-independent as is the case for $\delta = 0$. Using the fabricated size-dependent surface tension (Figure 3a), we recalculate the SDCE of fcc W nanoparticles shown in Figure 3b. The cohesive energy first decreases faster (region I), then remains size-independent (region II) for a while, and finally decreases (region III) again with decreasing particle size and is consistent with experimental data. A similar variation of cohesive energy with size has also been predicted for other systems.[43,44] However, a detailed experimental investigation for a large number of particle sizes is required to confirm this variation of cohesive energy with size. Further, the bulk cohesive energy can only be extrapolated from region I. In case of embedded nanoparticles, the coordination number can be assumed size-independent in the complete size range. Hence, the cohesive energy is expected to be linear with the inverse of the particle size. Cohesive energy is also expected to increase if there is an epitaxy between the nanoparticles and the matrix, and it is expected to be higher than the bulk value if the cohesive energy of the matrix material is higher than the nanoparticle materials.[4]

Recently, Yu et al. have shown that the variation of the SDCE is different for different structures of nanoparticles that assists in the evaluation of ST associated with nanoparticles.[43] It is well established for W nanoparticles that ST transition from bcc to fcc occurs for a particle size of 5−7 nm and from fcc to amorphous for a particle size of 1.0 nm.[45] The ST of W nanoparticles has been studied by X-ray diffraction (XRD) which cannot probe the crystal structure of 1.0-nm particles, and these particles can be regarded as clusters. Interestingly, three different size regimes can be realized from the SDCE curve of W (Figure 3b). Each regime corresponds to different crystal structures and, hence, the ST can easily be evaluated from the SDCE curve as demonstrated in Figure 3b. As the effective coordination number of fcc crystal is higher compared to bcc crystal, the slope of region II was expected to be larger. In contrast, the slope is almost zero and is due to the decrease in the surface tension of small particles.

In summary, it is shown that LDM can be used to understand SDCE of nanoparticles and clusters. On the basis of the experimental data and LDM, the SDCE in the complete size range is predicted. It is also shown that the variation of the surface tension with size is in accordance with the Tolman

equation where the Tolman length is size-dependent. The Tolman length increases with decreasing particle size, reaches a maximum, and then decreases if the particle size is reduced further. It is also confirmed that structural transition associated with the particle size can be evaluated from the SDCE.

References and Notes

(1) (a) Bre'chignac, C.; Busch, H.; Chuzac, Ph.; Leygnier, J. *J. Chem. Phys*. **1994**, *101*, 6992. (b) Naher, U.; Bjrnholm, S.; Frauendorf, S.; Garcias, F.; Guet, F. *Phys. Rep*. **1997**, *285*, 245. (c) Haberland, H.; Kornmeier, H.; Langosch, H.; Oschwal, M.; Tanner, G. *J. Chem. Soc., Faraday Trans*. **1990**, *86*, 2473. (d) Jarrold, M. F.; Honea, E. C. *J. Phys. Chem*. **1991**, *95*, 9181.

(2) (a) Borggreen, J.; Hansen, K.; Chandezon, F.; Dossing, T.; Elahajal M.; Echt, O. *Phys. Rev. A* **2000**, *62*, 013202. (b) Chandezon, F.; Bjornholm, S.; Broggreen, J.; Hansen, K. *Phys. Rev. B* **1997**, *55*, 5485.

(3) Nanda, K. K.; Behera, S. N.; Sahu, S. N. *J. Phys.: Condens. Matter* **2001**, *13*, 2861.

(4) Nanda, K. K.; Sahu, S. N.; Behera, S. N. *Phys. Rev. A* **2002**, *66*, 013208.

(5) Nanda, K. K.; Maisels, A.; Kruis, F. E.; Fissan, H.; Stappert, S. *Phys. Rev. Lett*. **2003**, *91*, 106102.

(6) Nanda, K. K.; Maisels, A.; Kruis, F. E.; Fissan, H.; Rellinghaus, B. unpublished.

(7) Xie, D.; Wang, M. P.; Qi, W. H. *J. Phys.: Condens. Matter* **2004**, *16*, L401.

(8) Qi, W. H.; Wang, M. P.; Xu, G. Y. *Chem. Phys. Lett*. **2004**, *372*, 632.

(9) Qi, W. H.; Wang, M. P. *Mater. Chem. Phys*. **2004**, *88*, 280.

(10) (a) Qi, W. H.; Wang, M. P. *J. Mater. Sci. Lett*. **2002**, *21*, 1743. (b) Qi, W. H.; Wang, M. P.; Hu, W. Y. *J. Phys. D: Appl. Phys*. **2005**, *38*, 1429.

(11) Jiang, Q.; Li, J. C.; Chi, B. Q. *Chem. Phys. Lett*. **2002**, *366*, 551.

(12) (a) Sun, C. Q.; Wang, Y.; Tay, B. K.; Li, S.; Huang, H.; Zhang, Y. B. *J. Phys. Chem. B* **2002**, *106*, 10701. (b) Sun, C. Q.; Li, C. M.; Bai, H. L.; Jiang, E. Y. *Nanotechnology* **2005**, *16*, 1290.

(13) Sun, C. Q.; Tay, B. K.; Zheng, X. T.; Li, S.; Chen, T. P.; Zhou, J.; Bai, H. L.; Jiang, E. Y. *J. Phys. Condens. Matter* **2002**, *14*, 7781.

(14) Toamneck, D.; Mukherjee, S.; Bennemann, K. H. *Phys. Rev. B* **1983**, *28*, 665.

(15) Kim, H. K.; Huh, S. H.; Park, J. W.; Jeong, J. W.; Lee, G. H. *Chem. Phys. Lett*. **2002**, *354*, 165.

(16) Lu, Z. Y.; Wang, C. Z.; Ho, K. M. *Phys. Rev. B* **2000**, *61*, 2329.

(17) Shvartsburg, A. A.; Jarrold, M. F. *Phys. Rev. Lett.* **2000**, *85*, 2530.

(18) Tolman, R. C. *J. Chem. Phys*. **1949**, *17*, 333.

(19) Flueli, M.; Borel, J. P. *J. Cryst. Growth* **1988**, *91*, 67.

(20) Herring, C. *Phys. Rev* **1951**, *82*, 87.

(21) Berry, C. R. *Phys. Rev*. **1952**, *88*, 596.

(22) de Planta, T.; Ghez, R.; Piuz, F. *Helv. Phys. Acta* **1964**, *37*, 74.

(23) Wasserman, H. J.; Vermaak, J. S. *Surf. Sci*. **1970**, *22*, 164.

(24) Montano, P. A.; Schulze, W.; Tesche, B.; Shenoy, G. K.; Morrison, T. I. *Phys. Rev. B* **1984**, *30*, 672.

(25) Hofmeister, H.; Thiel, S.; Dubiel, M.; Schurig, E. *Appl. Phys. Lett*. **1997**, *70*, 1694.

(26) Blackman, M.; Lisgarten, N. D.; Skimmer, L. M. *Nature* **1968**, *217*, 1245.

(27) Piuz, F. *Helv. Phys. Acta* **1964**, *37*, 620.

(28) Mays, C. W.; Vermak, J. S.; Kuhlmann-Wilsdorf, D. *Surf. Sci*. **1968**, *12*, 134.

(29) Solliard, C.; Flueli, M. *Surf. Sci*. **1985**, *156*, 487.

(30) Lamber, R.; Wetjen, S.; Schulz-Ekloff, G.; Baalmann, A. *J. Phys. Chem*. **1995**, *99*, 13834.

(31) Cluskey, P. D.; Newport, R. J.; Benfield, R. E.; Gurman, S. J.; Schmid, G. *Z. Phys. D* **1993**, *26*, S8.

(32) Sambles, J. R. *Proc. R. Soc. London A* **1971**, *324*, 339.

(33) Goldstein, A. N.; Echer, C. M.; Alivisatos, A. P. *Science* **1992**, *256*, 1425.

(34) Castro, T.; Reifenberger, R.; Choi, E.; Andres, R. P. *Phys. Rev. B* **1990**, *42*, 8548.

(35) Tyson, W. R.; Miller, W. A. *Surf. Sci*. **1977**, *62*, 267.

(36) Nanda, K. K. *Appl. Phys. Lett*. **2005**, *87*, 021909.

(37) Frenkel, A. I.; Hills, C. W.; Nuzzo, R. G. *J. Phys. Chem. B* **2001**, *105*, 12689.

(38) Rytkonen, A.; Valkealahti, S.; Manninen, M. *J. Chem. Phys*. **1997**, *106*, 1888.

(39) Li, Y.; Blaisten-Barojas, E.; Papaconstantopoulos, D. A. *Phys. Rev. B* **1998**, *57*, 15519.

(40) Pinto, A.; Pennisi, R.; Faraci, G.; Dagostino, G.; Mobilio, S.; Boscherini, F. *Phys. Rev. B* **1995**, *51*, 5315.

(41) Moody, M. P.; Attard, P. *J. Chem. Phys*. **2001**, *115*, 8967.

(42) (a) Bartell, L. S. *J. Phys. Chem. B* **2001**, *105*, 11615. (b) Granasy, L. *J. Chem. Phys*. **1998**, *109*, 9660. (c) Talanquer, V.; Oxtoby, D. W. *J. Phys. Chem*. **1995**, 99, 2865. (d) Koga, K.; Zeng, X. C. *J. Chem. Phys*. **1999**, *110*, 3466. (e) Nijmeijer, M. J.; Bruin, C.; van Woerkom, A. B.; Bakker, A. F. *J. Chem. Phys*. **1992**, *96*, 565. (f) Haye, M. J.; Bruin, C. *J. Chem. Phys*. **1994**, *100*, 556.

(43) Muilu, J.; Pakkenan, T. A. *Surf. Sci*. **1996**, *364*, 439.

(44) Yu, D. K.; Zhang, R. Q.; Lee, S. T. *Phys. Rev. B* **2002**, *65*, 245417.

(45) Oh, S. J.; Huh, S. H.; Kim, H. K.; Park, J. W.; Lee, G. H. *J. Chem. Phys*. **1999**, *111*, 7402.